HHS Public Access

Author manuscript

Nano Lett. Author manuscript; available in PMC 2020 June 04.

Published in final edited form as:

Nano Lett. 2019 March 13; 19(3): 2099–2105. doi:10.1021/acs.nanolett.9b00300.

Freeze-Drying To Produce Efficacious CPMV Virus-like Particles

Yi Zheng[†], **Parker W. Lee**[#,○], **Chao Wang**[†], **Linda D. Thomas**[‖,▽], **Phoebe L. Stewart**[‖,▽], **Nicole F. Steinmetz**[*,▽,§,⊥,‡,†], **Jonathan K. Pokorski**[*,#,†]

[†]Department of NanoEngineering, University of California San Diego, La Jolla, California 92093, United States

[‡]Department of Bioengineering, University of California San Diego, La Jolla, California 92093, United States

[§]Department of Radiology, University of California San Diego, La Jolla, California 92093, United States

[⊥]Moores Cancer Center, University of California San Diego, La Jolla, California 92093, United States

[‖]Department of Pharmacology and Cleveland Center for Membrane and Structural Biology, Case Western Reserve University, Cleveland, Ohio 44106, United States

[#]Department of Macromolecular Science and Engineering, Case Western Reserve University, Cleveland, Ohio 44106, United States

[▽]School of Medicine, Case Western Reserve University, Cleveland, Ohio 44106, United States

Abstract

In situ cancer vaccination that uses immune stimulating agents is revolutionizing the way that cancer is treated. In this realm, viruses and noninfectious virus-like particles have gained significant traction in reprogramming the immune system to recognize and eliminate malignancies. Recently, cowpea mosaic virus-like particles (VLPs) have shown exceptional promise in their ability to fight a variety of cancers. However, the current methods used to produce CPMV VLPs rely on agroinfiltration in plants. These protocols remain complicated and labor intensive and have the potential to introduce unwanted immunostimulatory agents, like lipopolysaccharides. This Letter describes a simple “post-processing” method to remove RNA from wild-type CPMV, while retaining the structure and function of the capsid. Lyophilization was able to eject encapsulated RNA to form lyo-eCPMV and, when purified, eliminated nearly all traces of encapsulated RNA. Lyo-eCPMV was characterized by cryo-electron microscopy single particle reconstruction to confirm the structural integrity of the viral capsid. Finally, lyo-eCPMV showed equivalent anticancer efficacy as eCPMV, produced by agroinfiltration, when using an

[*]**Corresponding Authors:** nsteinmetz@ucsd.edu, jpokorski@ucsd.edu.

[○]**Present Address:** P.W.L.: Beyond Meat, El Segundo, California 90245, USA.

Supporting Information

The Supporting Information is available free of charge on the ACS Publications website at DOI: 10.1021/acs.nanolett.9b00300.

Size exclusion chromatograms of unoptimized freezing conditions and curve fitting of lyo-CPMV (PDF)

The authors declare no competing financial interest.

invasive melanoma model. These results describe a straightforward method to prepare CPMV VLPs from infectious virions.

Graphical Abstract

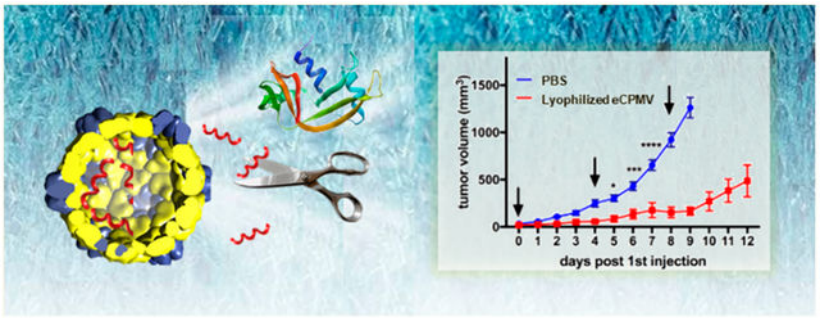

Keywords

Virus-like particle; immunotherapy; in situ vaccine; therapeutic protein; lyophilization

Viral nanoparticles (VNPs) are an emerging class of nanomaterials and have broad applications in materials science, agriculture, energy, and medicine.[1,2] The appeal of such particles is due to their near monodispersity, wide variety of shapes and sizes, and precise placement of functional groups for chemical or genetic modification.[3] The use of VNPs as platforms for immunoengineering is of particular interest, since their size generally lies between 20 and 300 nm, offering effective recognition by dendritic cells (DCs) or other antigen-presenting cells (APC).[4] In addition, the placement of epitopes occurs in a regular and repeating pattern around the capsid, thus activating the pathogen-associated molecular pattern (PAMP) response of the innate immune system.[5,6]

Virus-like particles (VLPs) are a subclass of VNPs lacking genomic material but retaining capsid structure and thus can elicit a similar immune response. The absence of nucleic acids makes them noninfectious and eliminates a potential uncontrolled immunostimulatory source, rendering VLPs ideal building blocks for immunotherapy.[7] As such, several VLP vaccines are in clinical trials or have been approved by the FDA. The most well-known is that of Gardasil, consisting of the major capsid protein of several human papilloma virus (HPV) subtypes.[8] VLPs have also been approved and are commonly used for vaccination against hepatitis B and hepatitis E.[9] Beyond this, a vast amount of resources has been dedicated toward preclinical and clinical trials of VLP vaccine candidates.[10] These novel therapies can be directed against the VLP itself or against antigens decorated about the VLP surface.[11,12]

One of the most sought-after areas in vaccine development is the development of cancer immunotherapies. A recent exciting innovation in cancer immunotherapy is the generation of *in situ* cancer vaccines, where an immunostimulatory agent is directly administered to a tumor site. The attributes of this class of therapy are that they are near universal immunotherapies, since no antigen is displayed. *In situ* vaccines elicit a strong memory antitumor

immune response by inducing immunogenic cancer cell death. This facilitates the release of tumor-associated antigens, increases the number of APCs, and enhances their activation to induce antitumor T cell responses, which results in systemic antitumor immunity.[13] One of the tools used for *in situ* vaccination are oncolytic viruses,[14] though the degree of immune responses they induce can relate to the particular virus used, the tumor burden, and the immunogenicity.[15] Additionally, safety concerns like infection and proliferation of oncolytic viruses cannot be eliminated since they are infectious.[16]

Recently, plant viruses emerged as *in situ* vaccines and showed exciting therapeutic effects in curing metastatic disease. In one example, a papaya mosaic virus had the capacity to activate the innate immune system and reduce tumor volume in a murine melanoma model.[17] Furthermore, VLPs derived from cowpea mosaic virus engineered to lack the viral RNA (eCPMV) achieve therapeutic activity in various poorly immunogenic murine tumor models, induce long-lasting antitumor immunity, and eradicate metastatic sites.[18] eCPMV has been further probed and was shown to be a privileged immunotherapy when compared to other plant-derived VLPs and VNPs.[19] eCPMV in combination with radiation was able to successfully treat advanced oral melanoma in companion pets.[20] Lastly, CPMV was formulated into slow release devices for intraperitoneal implantation and single-dose treatment of disseminated ovarian carcinomas.[21] eCPMV has clearly shown great utility and promise for cancer immunotherapy, giving us strong impetus to further this technology.

The current method used to produce eCPMV is the agroinfiltration of *Nicotiana bethamiana* plants using a plasmid-based expression system.[22] This methodology could potentially introduce immunostimulatory contaminants such as lipopolysaccharide (LPS) during bacterial infiltration.[23,24] Furthermore, scalable implementation of agroinfiltration is tedious, and yields are often significantly lower than wild-type CPMV production.[25] Chemical methods exist for RNA removal from wild-type CPMV; however, trace amounts of RNA remained present, fractionation was necessary to obtain mostly empty particles, and the harsh conditions denatured the capsid over time.[26] Here, we developed a streamlined method to produce eCPMV from native CPMV with a simple experimental setup and low demands for equipment and materials. A simple freeze-drying procedure ejected the RNA from the capsid, and RNase treatment was able to degrade the remaining nucleic acids to produce lyo-eCPMV. A series of characterization methods were carried out to show that the empty capsids maintained an intact capsid conformation. Furthermore, *in situ* injection of lyo-eCPMV was observed to have similar efficacy in tumor suppression as bacterially derived eCPMV. In sum, we present a straightforward method for the rapid production of eCPMV from native infectious CPMV.

Results and Discussion.

Lyo-eCPMV Production and Characterization.

This method was found empirically and serendipitously when we tried to lyophilize CPMV particles for storage and device manufacture. Removal of RNA from the capsid begins with a slow freeze of a CPMV aqueous solution at −20 °C. Temperature, time, and concentration are critical factors during the freezing step prior to lyophilization. Typical freezing procedures using liquid N_2 were unable to fully eject the RNA and resulted in increased

aggregation, decreasing the yield (Figure S1). Our optimized conditions were a slow freeze in a laboratory freezer (−20 °C, 4 days), followed by lyophilization. These conditions resulted in ideal capsid uniformity and complete removal of RNA. Furthermore, concentration during freezing is a critical factor in obtaining a sufficient yield. At high concentrations (>10 mg/mL), particles aggregate and significant fractions are unable to resuspend following lyophilization; however, dilute solutions of ~1 mg/mL lessen particle aggregation and maintain high yields. Following freezing, a four-day negative pressure lyophilization was the shortest time required in order to achieve complete dehydration and RNA ejection based on our observations. The resulting dry powder was a mixture of RNA, intact RNA-free particle, and a small amount of protein aggregates; the resulting mixture of components is referred to as lyo-CPMV. Lyo-CPMV was resuspended into buffered solution, and aggregates were removed by centrifugation and decanting. The last step in the lyo-eCPMV preparation is removal of genomic RNA. This was accomplished using RNase A, an extremely common endonuclease, to cleave the RNA into small fragments, which were easily removed using diafiltration with 100 kDa molecular weight cutoff centrifugal filters. Lyo-eCPMV was recovered at a yield of 0.5 mg of particles/1 g of infected leaf tissue, which was competitive with the yield of eCPMV as prepared by agroinfiltration.[27] (Figure 1).

Characterization of RNA Content of Lyo-eCPMV and Particle Purity.

Next, we used agarose gel electrophoresis to determine particle integrity and to test whether residual RNA would be associated with the VLPs following lyophilization (Figure 2A). The placement of the bands is determined by the absolute mobility of the viral nanoparticles, which is dependent on the presence of RNA within the capsid. VLPs with RNA have a higher electrophoretic mobility toward the anode based on the additional negative charge contribution from the RNA. Native CPMV is detectable under UV light after EtBr staining and under white light after Coomassie brilliant blue staining, indicating intact particles with encapsulated RNA. (The appearance of a double band can be explained by the two different electrophoretic forms of the virus.)[28] By contrast, lyo-CPMV shows “free” RNA with a high electrophoretic mobility that is not associated with the capsid protein; therefore, suggesting that the RNA was ejected during the lyophilization process. Native CPMV contains a bipartite RNA genome with RNA-1 of 5.9 kb and RNA-2 of 3.5 kb;[29–31] the fact that only one RNA band is observed may suggest that the RNA may be degraded, aggregated, or cannot be resolved under the conditions tested. Taken together, agarose gel electrophoresis gave a strong indication that RNA was ejected to form a nucleic acid-free VLP.

Further evidence of RNA removal can be found in UV-vis spectroscopy (Figure 2B); the encapsulated nucleic acids have a dominant absorbance peak at 260 nm, while absorbance at 280 nm is reflective of the protein capsid with a lesser contribution from the nucleic acids.[32] The ratio between these two absorbance intensities is indicative of RNA presence in the final material. Wild-type CPMV had a A_{260}/A_{280} ratio of 1.573, which correlated with the literature value of 1.57,[33] and suggested RNA encapsulation, as would be expected.[34] The A_{260}/A_{280} ratio of lyo-CPMV increased to 2.090, which is a result of RNA unfolding and ejection from the capsid. The unusually high ratio is likely further skewed due to insoluble protein precipitate. Finally, the absorbance ratio of lyo-eCPMV dramatically dropped to 0.804, indicating that nearly all RNA was removed. This value is slightly higher than the

literature value of eCPMV at 0.69,[33] which likely indicates the presence of trace nucleic acids either in the supernatant or encapsulated within lyo-eCPMV.[34]

Agarose gels only give comparative sizes based on the band position of known standards. Dynamic light scattering (DLS) and fast protein liquid chromatography (FPLC) were carried out to further characterize lyo-CPMV and lyo-eCPMV size and purity, respectively (Figure 3). DLS measurements show that the lyophilization and "post-processing" method have minimal impact on particle size and aggregation (Figure 3A). The DLS data indicate no obvious aggregates or collapsed protein subunits for wild-type CPMV, with a hydrodynamic radius of 16.4 nm. The hydrodynamic radius of lyo-CPMV is approximately the same (R_h = 14.5 nm), indicating that minimal aggregation occurred during the freeze-drying step. The hydrodynamic radius of lyo-eCPMV (14.9 nm) also showed little difference compared to wild-type CPMV. FPLC was used to determine particle purity (Figure 3B). Wild-type CPMV displays a single Gaussian peak centered at ~19 mL elution volume on a Sephacryl 1000 SF 10/300 size exclusion column. In contrast, lyo-CPMV exhibited a single peak centered at a slightly higher elution volume (~21 mL), which is no longer symmetric. This change can be attributed to released RNA remaining in the sample, since the genomic RNA is of reduced hydrodynamic volume relative to the capsid. The FPLC column was unable to fully resolve the capsid and ejected RNA; however, the asymmetric peak can be fit to two Gaussian distributions (Figure S2), one that corresponds to an intact capsid and another that is presumably genomic RNA. Further confirmation of this is evidenced by the high A_{260}/A_{280} ratio (>2.0), indicating a high concentration of nucleic acid. Once RNA was removed by nuclease treatment to form lyo-eCPMV, the A_{260}/A_{280} ratio was reversed and a stark decrease in total absorbance was seen indicating the absence of nucleic acids. The decrease in total absorbance of lyo-eCPMV is attributed to the significantly lower extinction coefficient at 280 nm of coat protein versus pure RNA (approximately 20-fold less). Furthermore, the elution volume returned to ~19 mL and regained symmetry, indicating intact viral capsids, with a minimal shoulder at lower elution volumes perhaps indicating a small population of aggregated species.

Cryo-EM Examination of Lyo-eCPMV.

The structural integrity of lyo-eCPMV particles was examined by cryo-electron microscopy (cryo-EM). As expected cryo-electron micrographs of wild-type CPMV particles show dark interiors, indicative of the presence of encapsulated RNA (Figure 4A).[35] In contrast, lyo-eCPMV particles have lighter interiors and appear to be empty (Figure 4B). The cryo-electron micrographs also suggest that the icosahedral capsids of lyo-eCPMV particles are largely well-formed and structurally intact. Single particle reconstruction was performed on a data set of ~16 600 lyo-eCPMV particle images collected on a 200 kV cryo-electron microscope with an energy filter and a DE20 direct electron detector. Classification with RELION[36] helped to select a relatively homogeneous subset of ~8000 particle images. Refinement of this subset produced a 17 Å resolution structure (Figure 5A). The lyo-eCPMV cryo-EM structure reproduces many of the structural features observed in a cryo-EM structure of naturally occurring eCPMV filtered to the same resolution (Figure 5B).[35]

The cryo-EM reconstruction of lyo-eCPMV shows slight perturbances in the capsid structure. Few reports have investigated the effects of lyophilization on viral capsids;[37] however, potential reasons for particle disruption can be inferred from literature regarding protein freeze-drying. During the freezing and drying step, the solution concentration drastically increases, and this can lead to changes in pH and osmolyte concentration.[38] During this process, acidic groups are typically protonated, disrupting salt bridges and leading to destabilization of biological structures. It is likely that this effect caused disruption between the genomic RNA and coat protein. Furthermore, as the osmolyte concentration increases, so too does the internal pressure within the viral capsid, potentially leading to swelling of the particle. It is likely these two effects both destabilize RNA binding and lead to ejection of the RNA from the capsid. Once rehydrated, the disrupted lyo-eCPMV capsid appears to bounce back into a structure that resembles that of naturally occurring eCPMV. Since CPMV does not have pores of sufficient size to allow the genomic RNA to be repackaged in solution, we hypothesize that the freeze-drying and rehydration act as a kinetic trap to exclude RNA from being repackaged.

In Situ Vaccination with Lyo-eCPMV.

The most critical part of our method to make lyo-eCPMV is its ability to remain as a potent *in situ* cancer vaccine. Given the structural similarity of lyo-eCPMV to naturally occurring eCPMV as observed by cryo-EM single particle reconstruction, we were optimistic that lyo-eCPMV would retain similar antitumor properties in the treatment of melanoma. To confirm efficacy, we used the same murine melanoma model, with which we had seen success with eCPMV.[18] C57BL/6J male mice were inoculated with B16F10 murine melanoma cells subcutaneously. Treatment was started once the tumor size reached 4–5 mm in the largest diameter. Tumors were injected directly with 100 μg of lyo-eCPMV at 0, 4, and 8 days. By day 4, significant differences were seen in tumor volume, and by day 8, the tumor volume of control mice was nearly an order of magnitude greater than lyo-eCPMV-treated animals. Mice treated with lyo-eCPMV particles had significantly delayed tumor progression, and survival was extended by ~100% (Figure 6). This result was similar to eCPMV treatment in previous studies,[18] which suggested lyo eCPMV has comparable immunostimulatory capabilities as eCPMV produced by agroinfiltration.

Conclusions.

eCPMV has seen enormous potential as an *in situ* cancer vaccine and has immunological traits that make it uniquely poised among viral nanoparticles to make a clinical impact. The methodology described within builds a bridge between those studying eCPMV for its curative properties and those that are interested in its downstream manufacturing. Freeze-drying is a standard method for preparing biopharmaceuticals, and particularly viral vaccines. Several reports have investigated the effects of freeze-drying on live viruses in the past and have observed varying levels of viral inactivation. This report, in contrast, shows complete inactivation and removal of genomic RNA from the capsid particle, rendering it non-infectious. Our methodology has the potential to replace agroinfiltration methods, thus eliminating potential bacterial contamination. In addition, our method starts with wild-type CPMV, which theoretically can be abundantly produced, and the postprocessing conditions

utilize equipment that is standard to the pharmaceutical industry. Given our results, the potential exists that careful optimization of freeze-drying procedures would replicate these results for other viral vaccines and should be further investigated. In sum, our results represent a novel way to prepare genome-free virus-like particles from infectious virions while maintaining efficacy.

Methods.

Materials.

Ultrapure water (Milli-Q, Bedford, MA) was used for all experiments. Bovine serum albumin (BSA), monosodium phosphate anhydrate, disodium phosphate heptahydrate, sodium chloride, tris base for molecular biology, acetate acid, PEG 8000, RNase A, and SimplyBlue SafeStain were purchased from Fisher Scientific. Bradford reagent was purchased from VWR Life Science. Agarose I, EDTA tetrasodium salt anhydrous, and ethidium bromide were purchased from Amresco. Sucrose was purchased from Acros Organics.

Instrumentation.

A VirTis Advantage EL-85 freeze-dryer (SP Scientific, Warminster, PA, USA) was used for lyophilization. Wyatt Möbiuζ was used to perform DLS. Samples were analyzed at 25 °C in plastic disposable cuvettes with a path length of 10 mm. Fast protein liquid chromatography (FPLC) was performed using a AKTAFPLC 900 chromatography system equipped with a Sephacryl 1000 SF 10/300 size exclusion column. The mobile phase used is 50 mM phosphate buffer, with 150 mM NaCl (pH 7.4) at a flow rate of 0.4 mL/min. Samples were injected at a concentration of approximately 0.7 mg/mL. Native gel electrophoresis was performed using 1.2% agarose gels in 1× Tris acetate/EDTA (TAE) buffer. TAE buffer (1×) was diluted from 50× TAE stock. (2 mol Tris-base, 0.9 mol acetate acid, and 0.05 mol EDTA in Milli-Q water made up 1 L of 50× TAE stock.) Running buffer is also 1× TAE buffer, and 10 μg of the sample was loaded.

CPMV Production and Purification.

Black-eyed peas (*Vigna unguiculata*) were inoculated with 100 ng/μL CPMV in 0.1 M potassium phosphate buffer (pH 7.0) and propagated for 18–20 days using established procedures.[38] Briefly, infected leaves were homogenized in a commercial blender in 0.1 M potassium phosphate buffer, pH 7.0. The homogenized mixture was clarified by centrifugation (15 000*g*, 20 min), followed by a 1:1 chloroform/*n*-butanol extraction to remove hydrophobic debris. The aqueous layer was precipitated using PEG6000 (4% w/v) and NaCl (0.2M), and the pellet was collected by centrifugation. The resulting pellet was resuspended in 0.1 M potassium phosphate buffer and purified using a 10–40% sucrose density gradient.

Lyo-eCPMV Production.

CPMV was first filtered into deionized water using a 100 K Amicon Ultra-4 centrifugal filter at 6000 rpm (Eppendorf 5810 centrifuge) at least 6 times in order to remove salts and low molecular weight impurities from the product. The filtered CPMV stock was then adjusted

to 1 mg/mL with deionized water and slowly frozen at −20 °C in a laboratory freezer for at least 4 days. The tray freeze-dryer was used with a shelf temperature of 25 °C and an ultimate chamber pressure of 5 μbar. The final lyophilized particles exhibited a slightly yellow flocculent appearance.

Lyophilized particles were resuspended in 1 mL of 0.1 M potassium phosphate buffer (pH 7.0) overnight. Resuspended particles were more turbid compared to the original CPMV suspension, indicating incomplete suspension of the original material. Centrifugation (Eppendorf 5424) was performed at 1000 rpm for 5 min to precipitate the turbid material. The supernatant was collected and adjusted to ~1 mg/mL as determined by the Bradford assay. RNase A was then added to the resuspended lyo-CPMV at a concentration of 50 μg/mL. The samples were vortexed and incubated at room temperature for 15 min with gentle mixing by vortex at the level of 1.5. Following RNase treatment, 100 K Amicon Ultra-4 centrifugal filters were used to remove RNase A and degraded RNA (6000 rpm in an Eppendorf 5810R, 0.1 M KP, pH 7). Filtration was performed at least 6 times to completely remove degraded RNA fragments. Finally, the recovered particles were centrifuged at 10 000 rpm (Eppendorf 5424) for 5 min to remove any particulate aggregates.

Cryo Specimen Preparation and Image Collection.

Three μL aliquots of lyophilized, RNase A-treated, and filtered CPMV (lyo-eCPMV) at 0.5 mg/mL were applied onto 300 mesh copper grids (Quantifoil R2/2) that were glow discharged for 20 s at 20 mA. Excess solution was blotted for 1 s with filter paper, and the grids were immediately plunged into liquid ethane using a ThermoFisher/FEI Vitrobot. Cryo-EM data was collected on a JEOL 2200 FS microscope (FEG, in-column energy filter) operated at 200 kV. Images were recorded on a Direct Electron DE 20 detector at a magnification of 60 000× corresponding to a pixel value of 1.12 Å. Each micrograph was generated by averaging 32 individual dose fractionated frames collected at a rate of 20 frames/s for 1.6 s with an accumulated total dose of 63.3 electrons/pixel. The frames were motion corrected and summed into a single micrograph and processed. The micrographs were collected with underfocus values in the range of 1.6–3.5 μm.

Image Processing and 3D Reconstruction.

Particle selection was performed using the EMAN2 software suite.[39] A set of 16 628 particle images was selected from 181 cryo-electron micrographs. The defocus and astigmatism values for each of the micrographs were estimated using CTFFIND 4.1.[40] The RELION 2.1 software suite was used for further image processing.[36] After the RELION 2D classification step, particle images in 40 out of 82 2D classes were selected for further processing (14 059 particle images selected). The cryo-EM structure of naturally empty eCPMV at 4.25 Å resolution was obtained from the Electron Microscopy Data Bank (EMD-3562)[35] and was used as a reference map during 3D classification. The CPMV reference map was rotated to the I1 symmetry orientation and low-pass filtered to 10 Å resolution. After the RELION 3D classification step, particle images in 1 of 10 3D classes were selected for independent refinement with RELION 3D autorefine. This class contains 8 135 particle images (58% of the total data set) and refined to 17 Å resolution (at the Fourier Shell Correlation 0.143 threshold). Images were created with UCSF Chimera.[41]

Cell Culture.

B16F10 cells (ATCC) were cultured in Dulbecco's modified Eagle's media (DMEM, Life Technologies) at 37 °C in a 5% CO_2 humidified atmosphere, supplemented with 10% (v/v) fetal bovine serum (FBS, Atlanta Biologicals) and 1% (v/v) penicillin-streptomycin (Life Technologies).

Immunization of mice.

All experiments were conducted in accordance with Case Western Reserve University's IACUC. Also, 1.25×10^5 B16F10 cells/30 μL of PBS was introduced intradermally into the right flank of a C57BL/6J male (Jackson Laboratory). Animals were observed closely, and tumor size was measured with digital calipers. Tumor volumes were calculated as $V = 0.5\ (a \times b^2)$; where a is the length and b is the width of the tumor. Once tumor size reached 4–5 mm in the largest diameter, mice were randomized to the experimental groups: PBS and lyo-eCPMV ($n = 4$). Then, 100 μg of lyo-eCPMV and sterile PBS were injected into tumors in a volume of 30 μL every 4 days for a total of 3 treatments. Animals were sacrificed when the tumors reached a volume > 1500 mm^3.

Supplementary Material

Refer to Web version on PubMed Central for supplementary material.

ACKNOWLEDGMENTS

This work was funded in part through grants by the National Institute of Health (NIH R21 EB024874 to J.K.P. and N.F.S. and NIH U01CA218292 to N.F.S.).

REFERENCES

(1). Hefferon KL Repurposing Plant Virus Nanoparticles. Vaccines 2018, 6, 11.

(2). Czapar AE; Steinmetz NF Plant viruses and bacteriophages for drug delivery in medicine and biotechnology. Curr. Opin. Chem. Biol 2017, 38, 108–116. [PubMed: 28426952]

(3). Pokorski JK; Steinmetz NF The Art of Engineering Viral Nanoparticles. Mol. Pharmaceutics 2011, 8, 29–43.

(4). Benne N; van Duijn J; Kuiper J; Jiskoot W; Slütter B Orchestrating immune responses: How size, shape and rigidity affect the immunogenicity of particulate vaccines. J. Controlled Release 2016, 234, 124–134.

(5). Irvine DJ; Hanson MC; Rakhra K; Tokatlian T Synthetic Nanoparticles for Vaccines and Immunotherapy. Chem. Rev 2015, 115, 11109–11146. [PubMed: 26154342]

(6). Gomes AC; Mohsen M; Bachmann MF Harnessing Nanoparticles for Immunomodulation and Vaccines. Vaccines 2017, 5, 6.

(7). Kushnir N; Streatfield SJ; Yusibov V Virus-like particles as a highly efficient vaccine platform: Diversity of targets and production systems and advances in clinical development. Vaccine 2012, 31, 58–83. [PubMed: 23142589]

(8). Bogani G; Leone Roberti Maggiore U; Signorelli M; Martinelli F; Ditto A; Sabatucci I; Mosca L; Lorusso D; Raspagliesi F The role of human papillomavirus vaccines in cervical cancer: Prevention and treatment. Crit. Rev. Oncol. Hematol 2018, 122, 92–97. [PubMed: 29458794]

(9). Ogholikhan S; Schwarz KB Hepatitis Vaccines. Vaccines 2016, 4, 6.

(10). Balke I; Zeltins A Use of plant viruses and virus-like particles for the creation of novel vaccines. Adv. Drug Delivery Rev 2018.

(11). Bachmann MF; Jennings GT Vaccine delivery: a matter of size, geometry, kinetics and molecular patterns. Nat. Rev. Immunol 2010, 10, 787–796. [PubMed: 20948547]

(12). Clarke BE; Newton SE; Carroll AR; Francis MJ; Appleyard G; Syred AD; Highfield PE; Rowlands DJ; Brown F Improved immunogenicity of a peptide epitope after fusion to hepatitis B core protein. Nature 1987, 330, 381–384. [PubMed: 2446137]

(13). Hammerich L; Binder A; Brody JD In situ vaccination: Cancer immunotherapy both personalized and off-the-shelf. Mol. Oncol 2015, 9, 1966–1981. [PubMed: 26632446]

(14). Harrington KJ; Puzanov I; Hecht JR; Hodi FS; Szabo Z; Murugappan S; Kaufman HL Clinical development of talimogene laherparepvec (T-VEC): a modified herpes simplex virus type-1-derived oncolytic immunotherapy. Expert Rev. Anticancer Ther 2015, 15, 1389–403. [PubMed: 26558498]

(15). Bartlett DL; Liu Z; Sathaiah M; Ravindranathan R; Guo Z; He Y; Guo ZS Oncolytic viruses as therapeutic cancer vaccines. Mol. Cancer 2013, 12, 103. [PubMed: 24020520]

(16). Chernajovsky Y; Layward L; Lemoine N Fighting cancer with oncolytic viruses. BMJ. 2006, 332, 170–172. [PubMed: 16424499]

(17). Lebel M-È; Chartrand K; Tarrab E; Savard P; Leclerc D; Lamarre A Potentiating Cancer Immunotherapy Using Papaya Mosaic Virus-Derived Nanoparticles. Nano Lett. 2016, 16, 1826–1832. [PubMed: 26891174]

(18). Lizotte PH; Wen AM; Sheen MR; Fields J; Rojanasopondist P; Steinmetz NF; Fiering S *In situ* vaccination with cowpea mosaic virus nanoparticles suppresses metastatic cancer. Nat. Nanotechnol 2016, 11, 295–303. [PubMed: 26689376]

(19). Murray AA; Wang C; Fiering S; Steinmetz NF In Situ Vaccination with Cowpea vs Tobacco Mosaic Virus against Melanoma. Mol. Pharmaceutics 2018, 15, 3700–3716.

(20). Hoopes PJ; Wagner RJ; Duval K; Kang K; Gladstone DJ; Moodie KL; Crary-Burney M; Ariaspulido H; Veliz FA; Steinmetz NF; et al. Treatment of Canine Oral Melanoma with Nanotechnology-Based Immunotherapy and Radiation. Mol. Pharmaceutics 2018, 15, 3717–3722.

(21). Czapar AE; Tiu BDB; Veliz FA; Pokorski JK; Steinmetz NF Slow-Release Formulation of Cowpea Mosaic Virus for In Situ Vaccine Delivery to Treat Ovarian Cancer. Adv. Sci 2018, 5, 1700991.

(22). Sainsbury F; Saxena P; Aljabali AAA; Saunders K; Evans DJ; Lomonossoff GP Genetic Engineering and Characterization of Cowpea Mosaic Virus Empty Virus-Like Particles. Methods Mol. Biol 2014, 1108, 139–153. [PubMed: 24243247]

(23). Liu P-F; Wang Y; Ulrich RG; Simmons CW; VanderGheynst JS; Gallo RL; Huang C-M Leaf-Encapsulated Vaccines: Agroinfiltration and Transient Expression of the Antigen Staphylococcal Endotoxin B in Radish Leaves. J. Immunol. Res 2018, 2018, 1.

(24). De Castro C; Molinaro A; Lanzetta R; Silipo A; Parrilli M Lipopolysaccharide structures from Agrobacterium and Rhizobiaceae species. Carbohydr. Res 2008, 343, 1924–1933. [PubMed: 18353297]

(25). Fuenmayor J; Gòdia F; Cervera L Production of virus-like particles for vaccines. New Biotechnol. 2017, 39, 174–180.

(26). Ochoa WF; Chatterji A; Lin T; Johnson JE Generation and Structural Analysis of Reactive Empty Particles Derived from an Icosahedral Virus. Chem. Biol 2006, 13, 771–778. [PubMed: 16873025]

(27). Machida K; Imataka H Production methods for viral particles. Biotechnol. Lett 2015, 37, 753–760. [PubMed: 25488519]

(28). Steinmetz NF; Evans DJ; Lomonossoff GP Chemical introduction of reactive thiols into a viral nanoscaffold: a method that avoids virus aggregation. ChemBioChem 2007, 8, 1131–1136. [PubMed: 17526061]

(29). Lomonossoff GP; Shanks M The nucleotide sequence of cowpea mosaic virus B RNA. EMBO J. 1983, 2, 2253–2258. [PubMed: 16453487]

(30). van Wezenbeek P; Verver J; Harmsen J; Vos P; van Kammen A Primary structure and gene organization of the middle-component RNA of cowpea mosaic virus. EMBO J. 1983, 2, 941–946. [PubMed: 6641721]

(31). Hesketh EL; Meshcheriakova Y; Dent KC; Saxena P; Thompson RF; Cockburn JJ; Lomonossoff GP; Ranson NA Mechanisms of assembly and genome packaging in an RNA virus revealed by high-resolution cryo-EM. Nat. Commun 2015, 6, 10113. [PubMed: 26657148]

(32). Yildiz I; Lee KL; Chen K; Shukla S; Steinmetz NF Infusion of imaging and therapeutic molecules into the plant virus-based carrier cowpea mosaic virus: Cargo-loading and delivery. J. Controlled Release 2013, 172, 568–578.

(33). Fraenkel-Conrat H Comprehensive Virology: Descriptive Catalogue of Viruses; Springer Science & Business Media, 2012.

(34). Glasel JA Validity of nucleic acid purities monitored by 260nm/280nm absorbance ratios. BioTechniques 1995, 18, 62–63. [PubMed: 7702855]

(35). Hesketh EL; Meshcheriakova Y; Thompson RF; Lomonossoff GP; Ranson NA The structures of a naturally empty cowpea mosaic virus particle and its genome-containing counterpart by cryo-electron microscopy. Sci. Rep 2017, 7, 539. [PubMed: 28373698]

(36). Scheres SHW RELION: Implementation of a Bayesian approach to cryo-EM structure determination. J. Struct. Biol 2012, 180, 519–530. [PubMed: 23000701]

(37). Hansen LJJ; Daoussi R; Vervaet C; Remon J-P; De Beer TRM Freeze-drying of live virus vaccines: A review. Vaccine 2015, 33, 5507–5519. [PubMed: 26364685]

(38). Cicerone MT; Pikal MJ; Qian KK Stabilization of proteins in solid form. Adv. Drug Delivery Rev 2015, 93, 14–24.

(39). Tang G; Peng L; Baldwin PR; Mann DS; Jiang W; Rees I; Ludtke SJ EMAN2: An extensible image processing suite for electron microscopy. J. Struct. Biol 2007, 157, 38–46. [PubMed: 16859925]

(40). Rohou A; Grigorieff N CTFFIND4: Fast and accurate defocus estimation from electron micrographs. J. Struct. Biol 2015, 192, 216–221. [PubMed: 26278980]

(41). Pettersen EF; Goddard TD; Huang CC; Couch SC; Greenblatt DM; Meng EC; Ferrin TE UCSF Chimera—A visualization system for exploratory research and analysis. J. Comput. Chem 2004, 25, 1605–1612. [PubMed: 15264254]

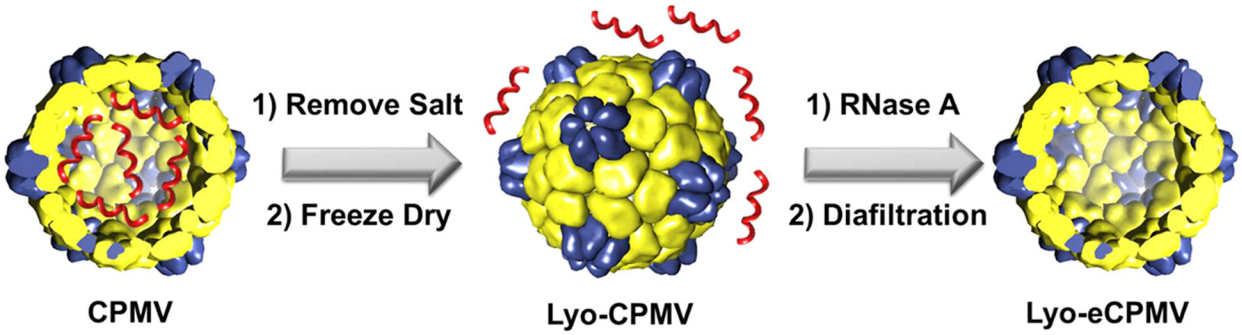

Figure 1.

Schematic of RNA removal from CPMV. Wild-type CPMV were freeze-dried, which resulted in intact lyo-CMPV. RNase A was used to remove genomic RNA and generate lyo-eCPMV.

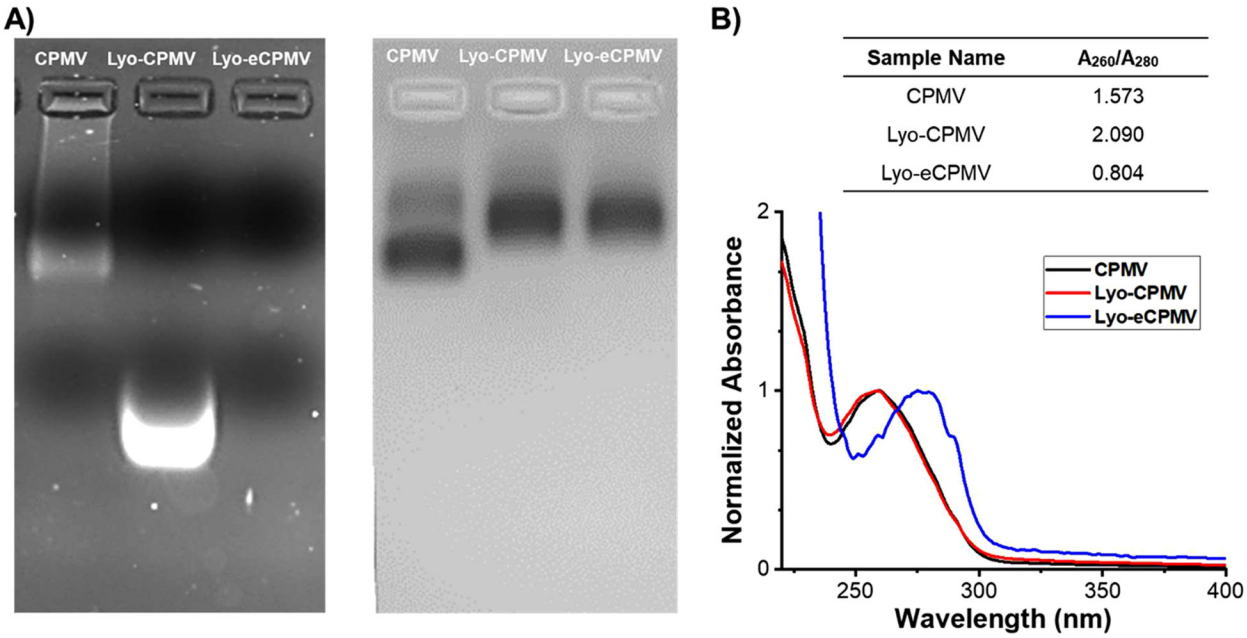

Figure 2.

Characterization of RNA removal. (A) 1% (w/v) agarose gel stained with ethidium bromide (left) and Coomassie brilliant blue (right). (B) UV-vis spectra and results for CPMV, lyo-CPMV, and lyo-eCPMV.

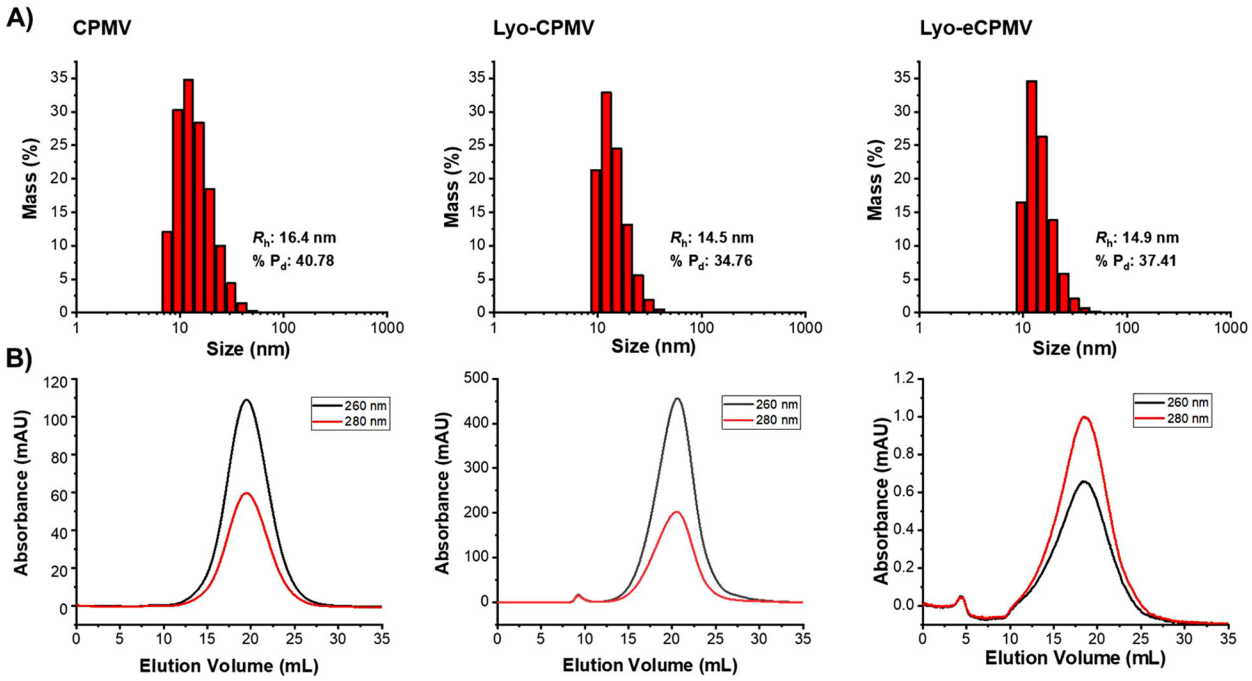

Figure 3.

Characterization of particle integrity. (A) Dynamic light scattering (DLS). DLS confirms that particles are intact and of appropriate size. The hydrodynamic radius (R_h) and the coefficient of variation (% Pd) are given for wild-type CPMV, lyo-CPMV, and lyo-eCPMV. (B) Fast protein liquid chromatography (FPLC). FPLC chromatograms for all stages of purification. Lyo-CPMV no longer has a Gaussian peak shape, indicating ejected RNA. Peak symmetry is recovered upon removal of free RNA for lyo-eCPMV.

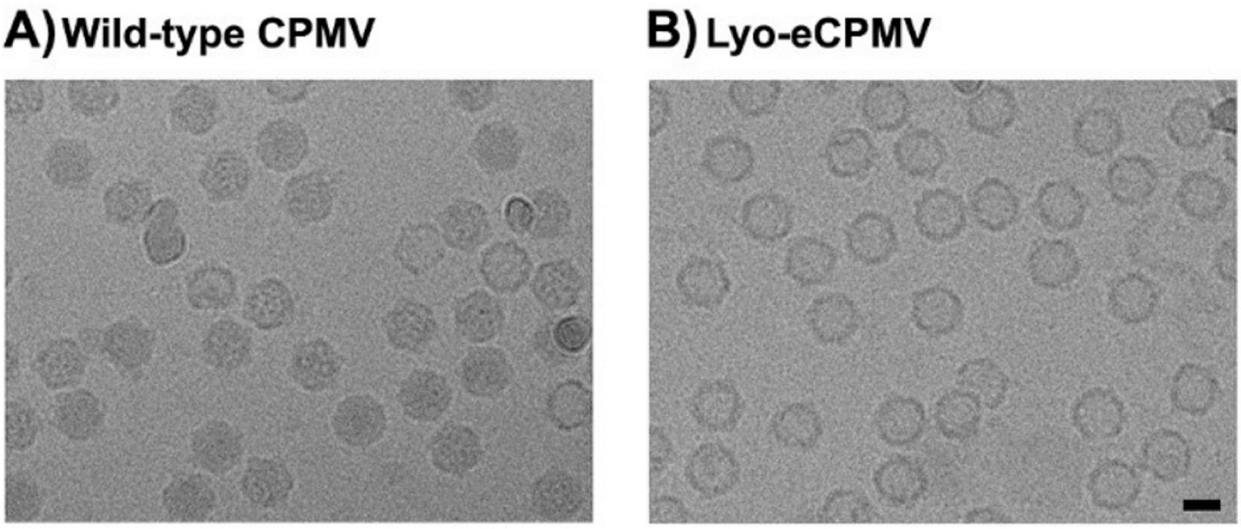

Figure 4.

Cryo-electron micrographs of wild-type CPMV and Lyo-eCPMV. (A) Wild-type CPMV particles appear dark in their interiors due to the presence of viral RNA. (B) Lyo-eCPMV particles have lighter interiors and appear to be empty. Both particles appear largely intact and nonaggregated. Scale bar = 200 Å.

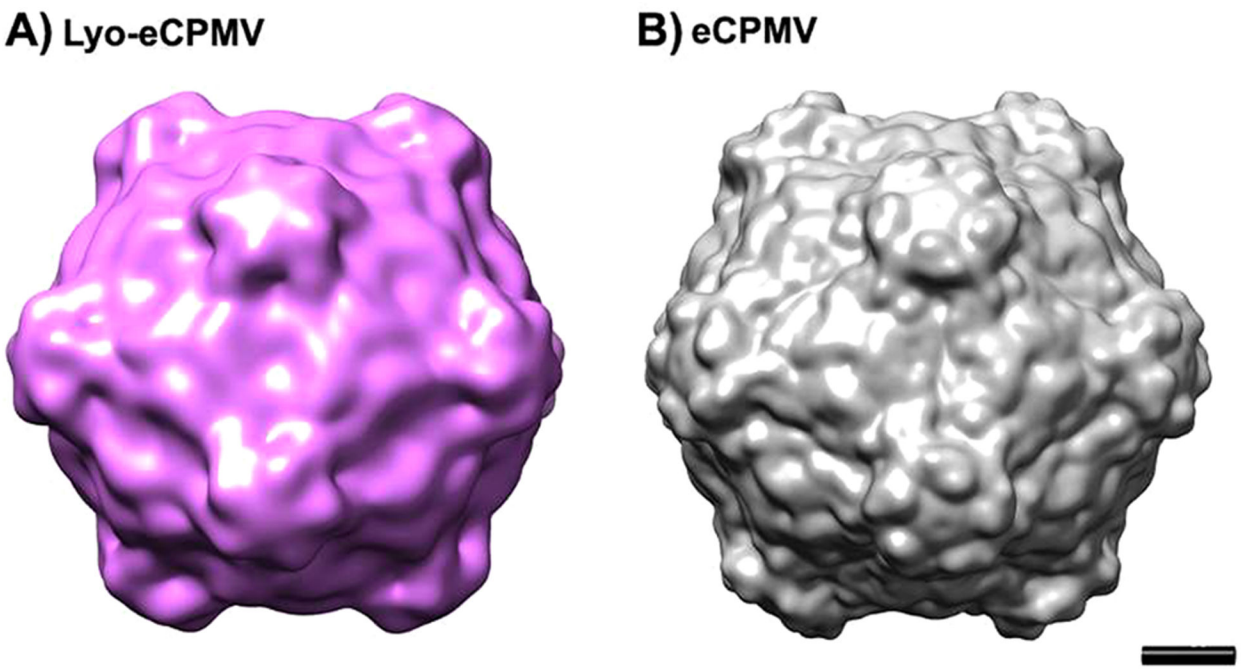

Figure 5.

Cryo-EM structure of lyo-eCPMV compared to the structure of naturally occurring eCPMV. (A) Cryo-EM structure of lyo-eCPMV at 17 Å resolution. (B) Cryo-EM structure of naturally occurring eCPMV (EMD: 3562)[35] shown filtered to 17 Å resolution. Scale bar = 50 Å.

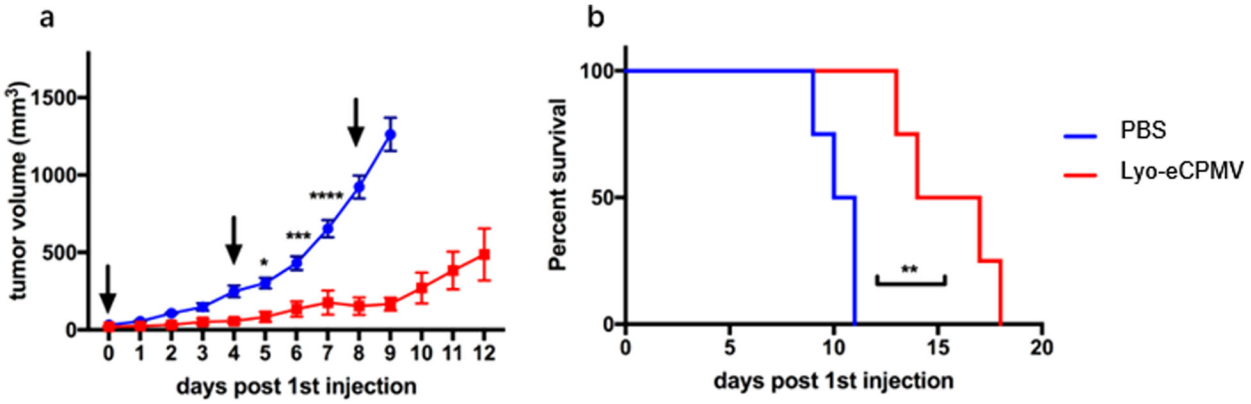

Figure 6.

In situ injection of lyo-eCPMV (lyo-eCPMV) inhibited B16F10 melanoma growth. Lyo-eCPMV (100 μg) were injected intratumorally on days 0, 4, and 8 ($n = 4$). (A) Tumor growth curves shown as a relative tumor volume. Data are means ± SEM. Statistical significance was calculated by two-way ANOVA with the Holm-Sidak test. *$p < 0.05$; ***$p < 0.0005$; ****$p < 0.0001$. Growth curves were stopped when the first animal of the corresponding group was sacrificed (tumor volume ≥ 1500 mm^3). (B) Survival rates of treated and control mice. Statistical significance was calculated by the Log-rank test. **$p < 0.01$.